ELSEVIER

Physica A 211 (1994) 399–410

PHYSICA A

Disorder effects on the effective dielectric response of a linear chain of polarizable spheres*

Cecilia Noguez, Rubén G. Barrera

Instituto de Física, Universidad Nacional Autónoma de México, Apartado Postal 20–364, 01000 México D.F., Mexico

Received 11 October 1993

Abstract

We perform a numerical simulation in order to calculate the dielectric response, to a long wavelength external field, for a linear chain of polarizable spheres embedded in a homogeneous host. The dielectric response is calculated within the dipolar, quasi-static approximation, and the position of each sphere is generated using three different types of disorder algorithms. The induced dipole moment on each sphere is calculated by solving a set of linear equations and using periodic boundary conditions. The imaginary part of the dielectric response as a function of frequency is shown and analyzed for the three types of disorder. These are also characterized through the calculation of the two-particle distribution function of the spheres.

1. Introduction

The study of the optical properties of inhomogeneous media has been an active field of research for more than over a century. At the beginning of this century J.C. Maxwell Garnett [1] calculated the effective dielectric response (EDR) of a system composed by spherical inclusions located at random positions within an otherwise homogeneous matrix. In his calculation, he assumed that the local field was uniform within each inclusion (dipolar approximation) and that all the spherical inclusions had the same induced dipole moment. This latter assumption is known nowadays as the mean field approximation (MFA), and is equivalent to the neglect of the local-field fluctuations. In the last decades, most of the efforts spent in the calculation of an EDR in granular systems with spherical inclusions have been directed to the removal of both of these assumptions [2].

* This paper was presented at the Third International Conference on Electrical Transport and Optical Properties of Inhomogeneous Media (ETOPIM 3), Guanajuato, Mexico, 9–13 August 1993. Selected papers of this conference were already published in Physica A 207 (1994) Nos. 1–3.

SSDI 0378-4371(94)00121-C

Up to now, the direct comparison between the different theoretical approaches and the experimental results has been a very painful task. This is due, essentially, to two facts:

(i) The samples do not resemble properly the idealized models used in the theoretical work. For example, in the samples the inclusions usually have a distribution of sizes and shapes, together with clustering effects.

(ii) Most of the experimental reports do not contain enough information about the actual statistical distribution of inclusions within the samples.

This latter point comes about, because most of the experimentalists intended to fit their data to either the Maxwell Garnett theory (MGT) or to the Bruggeman theory (BT), or to an extension of them in which the only information required about the microstructure of the system was the filling fraction of spheres. Thus this was the only recorded parameter. Nevertheless, it has been now recognized that it is quite fortuitous that the filling fraction were indeed the only microstructural information required in the MFA, and that this happens only in the very special case of spherical inclusions in 3D. As soon as one considers either a system of spheres located at random in 2D [6] or non-spherical inclusions in 3D [7], one finds that the calculation of the EDR in the dipolar, quasistatic, MFA requires an additional statistical information, namely, the two-particle distribution function of the inclusions. Furthermore, it can be shown that beyond the MFA, the two- and higher-particle distribution functions are a necessary input for the calculation of the EDR in the case of either spherical or non-spherical inclusions. Therefore, even an apparent disagreement between two sets of experimental results could not be legitimately resolved if the microstructure of the actual samples were not properly characterized.

Then, under these circumstances, one might say that the only fair test of the present theories is their comparison with numerical simulations which use the same model [3]. One might even be tempted to call these numerical results the "exact solution" of the model. Recently, Cichocki and Felderhof [4] have reported results of a numerical simulation for a system of spherical inclusions in 3D within the quasistatic, dipolar approximation. They calculate the spectral function of the EDR for 6 different filling fractions between 0.1 and 0.5. The configurations were generated by a Monte Carlo technique, with a hard sphere statistics, that is, the particle centers were distributed randomly apart from the nonoverlap condition. The spectra show a sharpening peak at the lower end of the spectrum as the filling fraction increases and they conjecture that it corresponds to a collective mode of the system. These results are certainly a main step forward towards the understanding of the dielectric response of granular systems; nevertheless one may wonder, how sensitive these results are, to different types of disorder. This question might be specially relevant, when one thinks of a real experimental situation, where the statistical distribution of inclusions is the result of a quite complicated preparation procedure, which could not be modeled, necessarily, by a system of hard spheres in thermal equilibrium.

At this respect, R.I. Cukier et al. [5] have reported results of numerical simulations for the imaginary part of the EDR for a system of conducting spherical inclusions in 3D but considering different kinds of disorder. They did it also within the dipolar approximation but only for a very low filling fractions f of spheres ($f = 0.03$). They find that the width of the absorption peak in the imaginary part of the EDR as a function of frequency, for spheres described by a Drude dielectric function, depends indeed on the type of disorder. Analogous results for high filling fractions are still lacking.

Here we perform a numerical simulation for the calculation of the EDR for a 1D chain of polarizable identical spheres. We do this within the quasistatic, dipolar approximation and we perform a systematic study for different types of disorder and for filling fractions covering the whole range, from the extreme-dilute to the close-packed limits. Our objective is twofold, first we want to study the properties of a 1D system due to the intrinsic interest that exists in the behavior of low-dimensional systems, and second, to shed some light into the possible dependence of the EDR on the type of disorder in systems in higher dimensions. Obviously, the computation time required for the simulation in a 1D chain is significantly smaller than in the corresponding 3D system. This allows us to perform the numerical calculations directly through matrix diagonalization and to study, in a systematic way, the fluctuations induced in the local field by the positional disorder of the spheres.

2. Formalism

We consider a linear chain of length L, lying along the Z-axis, with N ($\gg 1$) identical, non-overlapping, polarizable spheres of radius a and dielectric function $\epsilon_s(\omega)$, located at random positions $\{z_j\}$, within a homogeneous, dispersionless host with dielectric constant ϵ_h. The system is excited by an external electric field $\boldsymbol{E}^{\text{ext}}(\omega)$ oscillating with frequency ω and constant in space.

In the dipolar approximation, the local field induces in the ith sphere a dipole moment given by

$$\boldsymbol{p}_i = \alpha(\omega)\left\{\frac{\boldsymbol{E}_i^{\text{ext}}}{\epsilon_h} + \sum_{j=1}^{N} \boldsymbol{t}_{ij} \cdot \boldsymbol{p}_j\right\}, \tag{1}$$

where $\alpha(\omega) = a^3[\epsilon_s(\omega) - \epsilon_h]/[\epsilon_s(\omega) + 2\epsilon_h]$ is the effective polarizability of an isolated sphere within the host,

$$\boldsymbol{t}_{ij} = \frac{3\hat{\boldsymbol{R}}_{ij} \cdot \hat{\boldsymbol{R}}_{ij} - \boldsymbol{1}\delta_{ij}}{R_{ij}^3} \tag{2}$$

is the quasistatic dipole–dipole interaction tensor, and $R_{ij} = |\boldsymbol{R}_i - \boldsymbol{R}_j|$. For a linear chain $\hat{\boldsymbol{R}}_{ij} = (0, 0, 1)$.

The relation between the $\{\boldsymbol{p}_i\}$ and the *average* or *macroscopic* fields is given through

$$\boldsymbol{P} = n\langle \boldsymbol{p}_i \rangle = n\langle \boldsymbol{p} \rangle \,, \tag{3}$$

where $\boldsymbol{P}$, the *macroscopic* polarization field, is the dipole moment per unit volume, $n = N/(\pi a^2 L)$ is the number volume density of spheres, and $\langle \cdots \rangle$ means ensemble average. We assume that the ensemble is homogeneous, thus the average $\langle \boldsymbol{p}_i \rangle$ is independent of i. Here the volume of the system is chosen as a cylinder of radius a and length L.

Our purpose is the calculation of the *external* dielectric susceptibility tensor $\boldsymbol{\chi}_{\text{ext}}$, which relates the *macroscopic* polarization field with the *external* electric field, that is

$$\boldsymbol{P} \equiv \boldsymbol{\chi}_{\text{ext}} \cdot \boldsymbol{E}^{\text{ext}} \,. \tag{4}$$

We do this, by first generating the positions $\{z_i\}$ of the spheres along the chain with a certain type of disorder algorithm, then one solves Eq. (1) for $\{\boldsymbol{p}_i\}$ by matrix inversion and finally an ensemble average is taken over an ample set of chain configurations.

Edge effects due to the finite length of the chain are removed by using periodic boundary conditions. That is, given a finite set of positions $\{z_i\}$ in a chain, one constructs a unit cell of length L with $N-1$ spheres and then one takes an infinite number of unit cells locating the first sphere always in the same position, for example $z_1 = 0$. The distance between any pair of spheres in the infinite chain is given by

$$R_{ij}^{\mu\mu'} = |(z_i + \mu L) - (z_j + \mu' L)| = |z_{ij} + \sigma L| \,, \tag{5}$$

where μ denotes the cell, z_{ij} is the distance between two spheres in the same cell and σ can take any integer value.

The dipole–dipole interaction tensor $\boldsymbol{t}_{ij}$ for the infinite chain is diagonal in the coordinate system we have chosen, and can be now written as

$$\boldsymbol{t}_{ij} = \sum_{\sigma=-\infty}^{\infty} \frac{\boldsymbol{c}}{|z_{ij} + \sigma L|^3} \,, \tag{6}$$

where $\boldsymbol{c} = \text{diag}(-1, -1, 2)$. By performing the sum over all unit cells one gets

$$\boldsymbol{t}_{ij} = \frac{\boldsymbol{c}}{|z_{ij}|^3} + \sum_{\sigma=-m}^{m} \frac{\boldsymbol{c}}{|\sigma L|^3} \frac{1}{|1 + z_{ij}/\sigma L|^3} + \frac{2\boldsymbol{c}}{L^3}\left(\zeta(3) - \sum_{\sigma=1}^{m} \frac{1}{\sigma^3}\right) + \frac{12\boldsymbol{c} z_{ij}^2}{L^5}\left(\zeta(5) - \sum_{\sigma=1}^{m} \frac{1}{\sigma^5}\right) + \cdots \,, \tag{7}$$

where m is an integer, appropriately chosen to get quick convergence, and $\zeta(n)$ is the Riemann zeta function.

We now substitute this expression into Eq. (1) with $m = 2$ (which yields good convergence) and calculate the induced dipole moment in each sphere $\{\boldsymbol{p}_i\}$ by

solving a set of linear equations through the inversion of a $N \times N$ matrix. The average over each configuration l is calculated as $[\bar{P}]_l = (1/N) \sum_{i=1}^{N} P_i$ and the average over all configurations M is then

$$\langle P \rangle = \frac{1}{M} \sum_{l=1}^{M} [\bar{P}]_l \,. \tag{8}$$

Finally, the *external* susceptibility is obtained using Eq. (4).

First, we consider the *ordered* distribution, where the separation between spheres is the same, and then we consider distributions with three different kinds of disorder:

In disorder A, $N-1$ random positions are generated within the unit cell and the centers of the spheres are located on these sites with the only restriction that they do not overlap.

In disorder B, the first sphere is located at the edge of the unit cell and $N-1$ equidistant sites are defined within the cell. The next sphere is randomly located between the first sphere and the second site, the next one between the second sphere and the third site and so on.

In disorder C, the first sphere is located at the edge of the unit cell and $N-1$ equidistant sites are defined within the cell. Lets call s_0 the distance between these sites and then locate the k-th sphere randomly within an interval $2\delta s_0$ around the k-th site. The parameter $0 \leqslant \delta \leqslant \frac{1}{2}$ serves as a measure of the disorder, for example, $\delta = 0$ corresponds to the ordered case and $\delta = \frac{1}{2}$ to the maximum allowed disorder of this type.

The choice of these types of disorder has nothing in particular, the idea is simply to illustrate the sensitivity of the dielectric response to a specific type of disorder algorithm.

3. Results

We consider a system of metallic spheres with a Drude dielectric function with plasma frequency ω_p and an electronic relaxation time $\tau = 10^3/\omega_p$. The spheres are embedded in a homogeneous medium with a dispersionless dielectric constant $\epsilon_h = 2.37$ (gelatin). Results are presented for the imaginary part of the external susceptibility $\mathrm{Im}\, \chi_{ext}$ as a function of frequency, for each kind of disorder (A, B, C) discussed above. The peaks in $\mathrm{Im}\, \chi_{ext}$ correspond to the resonance frequencies of the collective electromagnetic modes of the system which are optically active; we will call these peaks, *absorption* peaks, and $\mathrm{Im}\, \chi_{ext}^{\mu\mu}(\omega)$, the *absorption* spectra. By optically active one means modes which can be excited by a long wavelength external field. As is well known, in the ordered case and for

$\tau \to \infty$, the imaginary part of the diagonal components of the susceptibility are delta functions. This means that there is only a single optically-active mode which can be excited for each direction (x, y, or z) of the external field. On the other hand, in the presence of disorder there is a broadening of the absorption peaks even for $\tau \to \infty$. What happens is that there are now disorder-induced fluctuations in the dipole moments of the spheres, enabling the existence of new optically-active modes which span a continuous range of frequencies. In order to illustrate this behavior, we have taken here $\tau = 10^3/\omega_p$, which is big enough to yield very narrow peaks in the ordered case. The number of spheres N depends on the filling fraction $f = 2Na/L$, where $L/a \sim 10^3$, and the ensemble averages are performed, typically, over $M \sim 100$ configurations.

In Figs. 1, 2 and 3 we show the results of the numerical simulation for Im $\chi^{zz}_{ext}(\omega)$, plotted as a function of $\Omega \equiv \omega/\omega_p$, for filling fractions $f = 0.3$, 0.5, and 0.8, respectively, and for the three types of disorder A, B, and C, discussed above. For disorder C we have set $\delta = \frac{1}{2}$. In these figures we take as a reference, the resonance frequency of the isolated sphere given by $\Omega_{i.s.} \equiv \omega_{i.s.}/\omega_p = 0.4174$, and the resonance frequency $\Omega_o \equiv \omega_o/\omega_p$ of the ordered case at the corresponding filling fraction. We mark them with vertical lines and denote them with i.s. and o respectively. We recall that the isolated resonance of the ordered array Ω_o corresponds to the one obtained for a disordered system with the same filling fraction using the *mean field* approximation. On the other hand, in Fig. 4, we show the corresponding results for Im $\chi^{xx}_{ext}(\omega)$ for disorder A and filling fractions $f = 0.3, 0.5$, and 0.8.

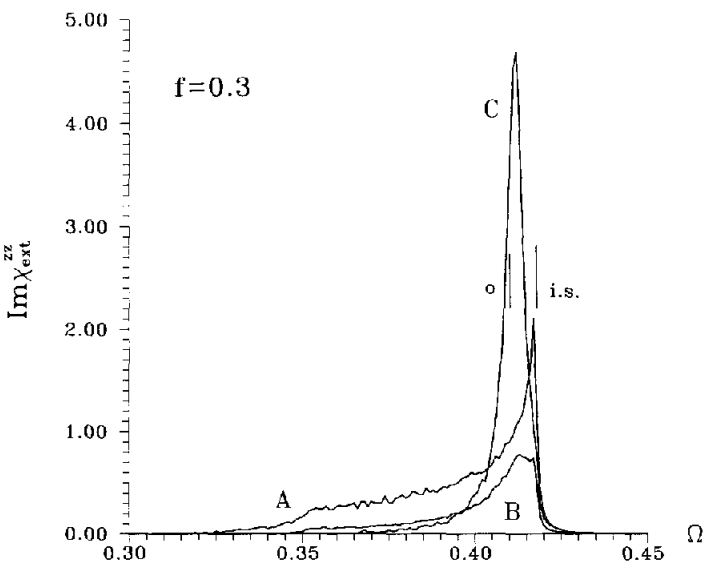

Fig. 1. Imaginary part of χ^{zz}_{ext} as a function of the reduced frequency $\Omega = \omega/\omega_p$ for disorder of type A, B and C, and filling fraction $f = 0.3$. The vertical lines mark the position of the resonance frequencies of the isolated sphere (i.s.) and the ordered array (o).

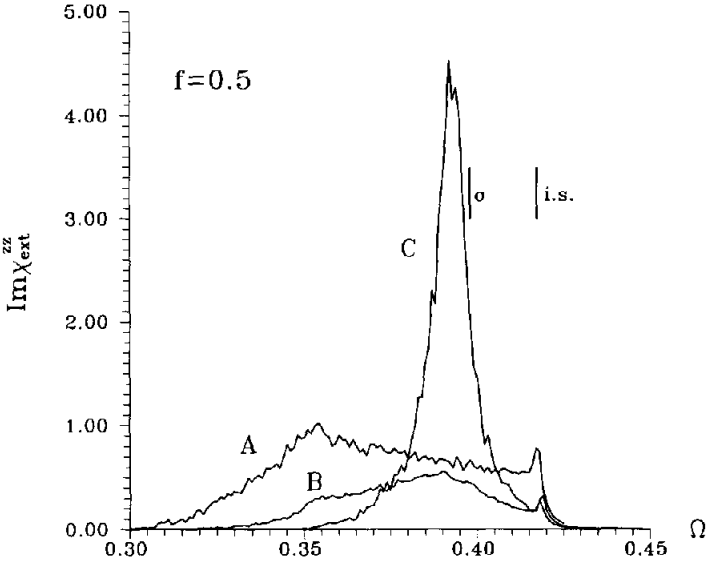

Fig. 2. Imaginary part of χ_{ext}^{zz} as a function of the reduced frequency $\Omega = \omega/\omega_p$ for disorder of type A, B and C, and filling fraction $f = 0.5$. The vertical lines mark the position of the resonance frequencies of the isolated sphere (i.s.) and the ordered array (o).

A special characteristic of this 1D system, which facilitates the analysis, is that the induced dipolar field of every neighboring sphere, at any given sphere site, points always parallel and along (opposite to) the external field when this field is

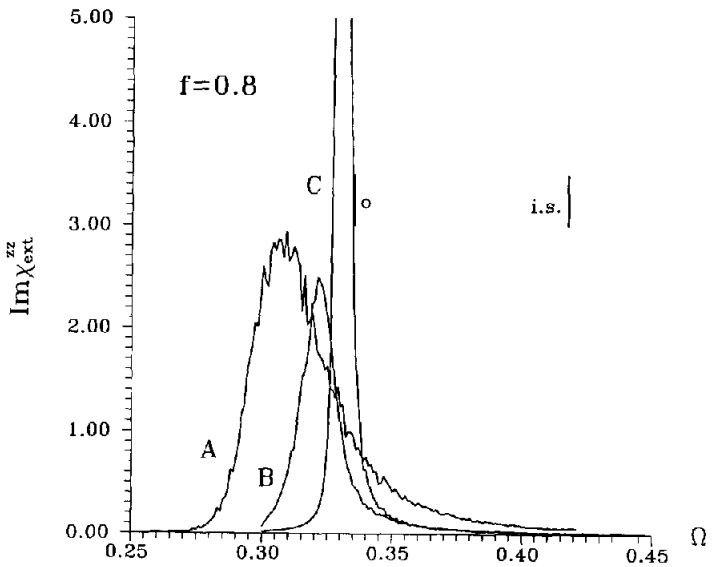

Fig. 3. Imaginary part of χ_{ext}^{zz} as a function of the reduced frequency $\Omega = \omega/\omega_p$ for disorder of type A, B and C, and filling fraction $f = 0.8$. The vertical lines mark the position of the resonance frequencies of the isolated sphere (i.s.) and the ordered array (o).

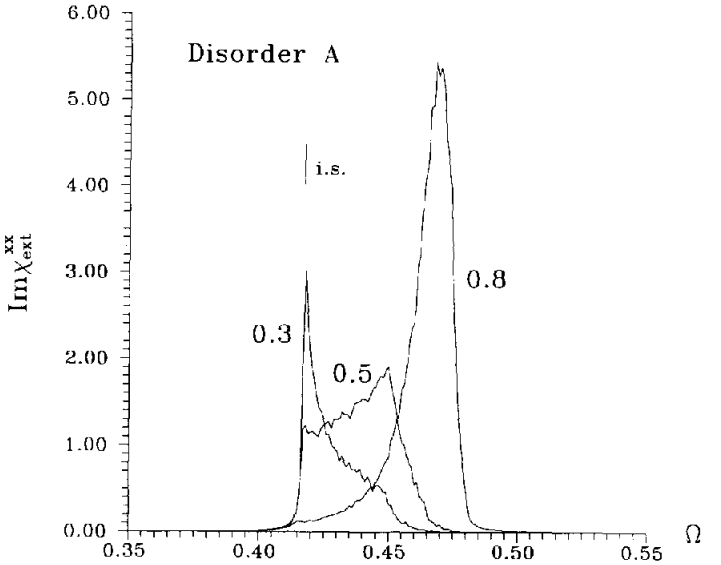

Fig. 4. Imaginary part of χ_{ext}^{zz} as a function of the reduced frequency $\Omega = \omega/\omega_p$ for disorder of type A and filling fractions $f = 0.1$, 0.3 and 0.8. The vertical lines mark the position of the resonance frequency of the isolated sphere (i.s.).

parallel (perpendicular) to the chain. This means that the local field, at any sphere site, is *always* greater (smaller) than the external field. As a consequence, the frequencies of the normal modes of the system are *always* softened (stiffened), that is, red-shifted (blue-shifted) with respect to the resonance frequency $\Omega_{i.s.}$ of the isolated sphere. The shift increases when the filling fraction increases. Thus $\Omega_{i.s.}$ becomes an upper (lower) limit in the spectra. The lower (upper) limit is the frequency $\Omega_L \equiv \omega_L/\omega_p$ ($\Omega_U \equiv \omega_U/\omega_p$) of the mode L(U) at which the local field is the largest (smallest) possible field at every sphere site, and this happens in the configuration where the spheres are as close as possible to each other for a given filling fraction. It is obvious that this frequency Ω_L (Ω_U) should be larger (smaller) than Ω_c, the one corresponding to the close-packed configuration $f = 1$, but smaller (greater) than $\Omega_2 \equiv \omega_2/\omega_p$, the one corresponding to a system of only two spheres at the minimum separation $2a$. In our case of spheres embedded in gelatin this corresponds to $0.2538 \leq \Omega_L \leq 0.3511$ ($0.4651 \leq \Omega_U \leq 0.5121$) and the absorption spectrum is then limited to the frequency range $\Omega_L \leq \Omega \leq \Omega_{i.s.}$ ($\Omega_{i.s.} \leq \Omega \leq \Omega_U$).

Furthermore, since the profile of the absorption spectra mirrors the density of states of the normal modes of the system, one can understand the difference in shape of these spectra in terms of how the probability of finding different kinds of modes changes at various filling fractions. For example, for low filling fractions the spheres are, on the average, well separated from each other and one expects a larger probability of finding mode configurations with frequencies closer to $\Omega_{i.s.}$ than to $\Omega_L(\Omega_U)$. This would yield spectra with a peak on the high (low)

frequency side and a tail in the low (high) frequency one. On the contrary, for high filling fractions one expects a larger probability of finding mode configurations with frequencies closer to Ω_L than to $\Omega_{i.s.}$, yielding spectra with a peak on the low (high) frequency side and a tail in the high (low) frequency one. Nevertheless for $f \simeq 1$ the system is becoming ordered, thus the spectra should narrow and narrow in order to become finally a delta function at $f = 1$. At intermediate filling fractions the shape of the spectra should represent a transition between the one at low f and the one at high f.

Looking at Figs. 1, 2 and 3, we see that the spectrum falls within the predicted frequency range for an external field parallel to the chain, and that the anticipated behavior discussed above is well illustrated in curves A and B. At $f = 0.3$ they are highly asymmetric with a long tail on the low frequency side and a sharp edge at $\Omega = \Omega_{i.s.}$. At $f = 0.8$ their peaks are also asymmetric but their shape is now reversed; the long tail is at the high frequency side and there is an edge, not as sharp, at the low frequency side. A transition between these two situations occurs at $f = 0.5$ where the profiles have two peaks: a small and narrow peak close to $\Omega_{i.s.}$ and a rather broad one at lower frequencies. On the other hand, curve C peaks close to Ω_0 for the three filling fractions shown here. This behavior is obviously inherited from the one associated to the ordered configuration which serves as a seed for the generation of disorder. Therefore, disorder generated in this way inhibits the appearance of low-frequency configurations. This can be more clearly seen when one chooses the parameter δ less than $\frac{1}{2}$ and one gets, as expected, an absorption peak with a profile more and more similar to the ordered case. Here we chose $\delta = \frac{1}{2}$ because it represents the maximum allowed disorder of this type. In case the external field lies perpendicular to the chain, one can see in Fig. 4, that the profile of the absorption spectra also follows the behavior predicted above. Although the results for disorder of types B and C are not shown in this figure, the corresponding behavior of the profile of $\mathrm{Im}\,\chi^{xx}_{ext}(\omega)$ for different filling fractions, as compared with disorder of type A, is analogous to the one shown in Figs. 1–3.

Nevertheless, the main message conveyed by these figures is the great sensitivity of the effective dielectric response to the type of disorder. In each of the first three figures, the curves denoted with A, B, and C are markedly different. The profile of curve C is always distinctly taller, narrower and more symmetric than the corresponding ones of curves A and B. The noise present in all these curves is *numerical* noise and can be smoothened out by averaging over a larger number of configurations. For large filling fractions ($f > 0.3$) the calculations were done on a CRAY machine and our only limitation was computer time.

It is also interesting to point out that an average over random orientations of the chain would lead to absorption spectra given by $\frac{1}{3}\mathrm{Im}\,\chi^{zz}_{ext}(\omega) + \frac{2}{3}\mathrm{Im}\,\chi^{xx}_{ext}(\omega)$. It is then immediately seen that these spectra show two characteristic peaks, one below and the other one above $\Omega_{i.s.}$. This double-peak structure is also present in the calculated spectra of the solid-angle-averaged absorption coefficient of an

ordered chain of polarizable spheres [8]; this result was used to explain the double-peak in the experimental absorption spectrum of gold colloids.

One way to characterize the different types of disorder is through the two-particle distribution function $g(R)$. Given a sphere at z_1, $g(R)$ is proportional to the probability of finding another sphere along the chain at a distance R from z_1, and normalized such that $g(R\to\infty)=1$. We calculated $g(R)$ numerically for the types of disorder discussed above. In this case, in order to obtain a bigger signal to noise ratio, it was necessary to average over a larger number of configurations, typically ≈5000. In Fig. 5 we plot $g(R)$ as a function of R, for $f=0.5$ and the three types of disorder A, B, and C, while in Fig. 6 we plot $g(R)$ as a function of R for $f=0.8$ and disorders of type A and B; disorder of type C was not included here for the sake of a clearer figure. In the ordered case we have that $g(R)$ is a set of delta functions located at the sphere positions. Looking at Figs. 5 and 6 one observes that when the spheres are now moved randomly around these positions, as in disorder of type C, the delta functions are broadened. On the other hand, when the disorder in the system is generated through algorithm A, the two-particle distribution function shows big oscillations at very short distances, which decay relatively soon to an asymptotic value g_A. Here the value of g_A is different from 1 due to the finite number of particles. For disorder B, $g(R)$ has small oscillations around g_A, which extend almost undamped to very large distances. The maxima of these oscillations are at the sphere positions in the ordered array as illustrated also in Figs. 5 and 6. From these figures we can see that disorder of

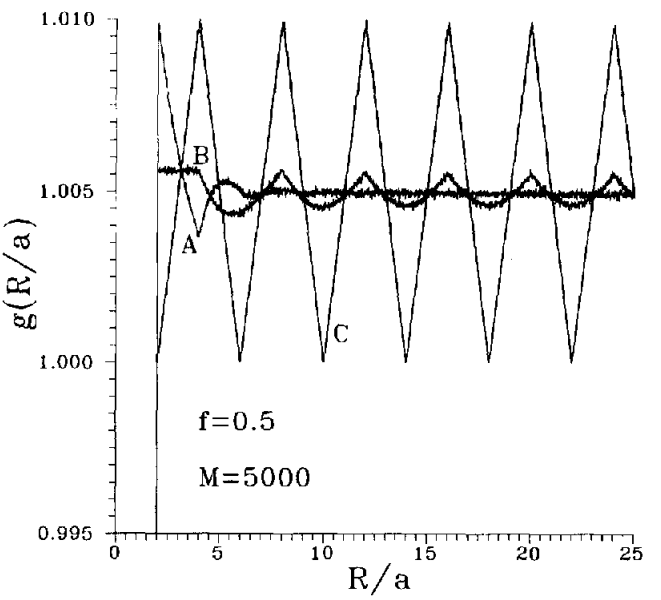

Fig. 5. The two-particle distribution function $g(R/a)$ as a function of R/a, for the three types of disorder A, B and C, and a filling fraction $f=0.5$. The ensemble average was done over 5000 configurations.

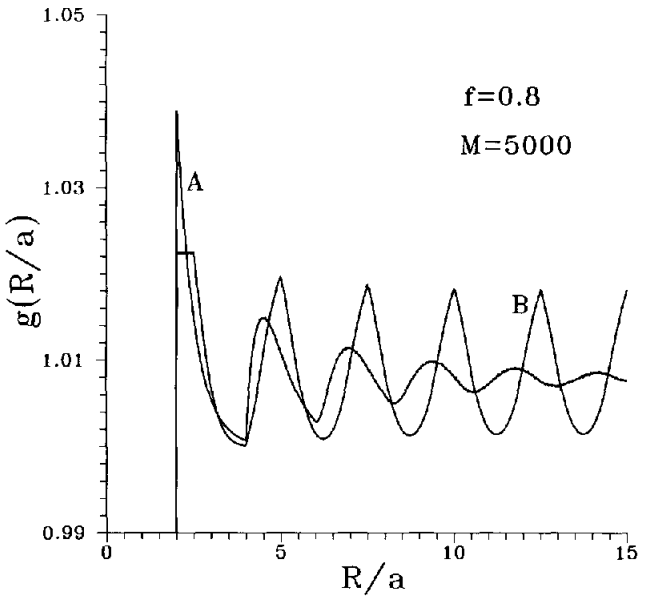

Fig. 6. The two-particle distribution function $g(R/a)$ as a function of R/a, for disorder of type A, and B, and a filling fraction $f = 0.8$. The ensemble average was done over 5000 configurations.

type B seems to be a transition between the disorders of types A and C. This seems to be also the case when looking back at the absorption spectra of Figs. 1–3.

4. Conclusions

In this work we perform a numerical simulation to calculate the external susceptibility of a 1D chain of polarizable spheres located at random positions. We do this for three different types of disorder, and we present results for three different filling fractions. The main result is the great sensitivity of the dielectric response to the specific choice of the disorder algorithm. We calculate the imaginary part of the external susceptibility as a function of frequency (absorption spectra) and we present an intuitive explanation of how the shape of its profile changes as the filling fraction increases. This is done in terms of the change in the density of states of low and high frequency modes at different filling fractions.

In a 3D system, the local field at a sphere site, coming from a neighboring sphere, would have, in general, components both parallel and perpendicular to the external field. Therefore it is not obvious to know in advance in which direction the local field will point, on the different sphere sites. Nevertheless, it is interesting to notice that the behavior of the profile, as the filling fraction increases, of the absorption spectra for a Monte Carlo hard-sphere disorder in 3D

[4], follows very much the same pattern as Im $\chi^{zz}_{ext}(\omega)$ for disorder of type A as calculated here.

Acknowledgements

We acknowledge illuminating discussions with Pedro Villaseñor-González, Ron Fuchs and W. Luis Mochán. This work was partially supported by Dirección General de Asuntos del Personal Académico and Coordinación General de Estudios de Posgrado of the Universidad Nacional Autónoma de México (Mexico), under grants IN-102493 and PADEP 003004, respectively.

References

[1] J.C. Maxwell Garnett, Philos. Trans. R. Soc. London 302 (1904) 385.
[2] J.C. Garland and D.B. Tanner, eds., Electrical Transport and Optical Properties of Inhomogeneous Media, ETOPIM, AIP conference Proceedings (American Institute of Physics, New York 1978);
R.G. Barrera and W.L. Mochán, eds., Electrodynamics of Interfaces and Composite Systems, Advanced Series in Surface Science, Vol. 4 (World Scientific, Singapore, 1988);
J. Lafait and D.B. Tanner, eds., ETOPIM2, Proceedings of the Second International Conference on Electrical Transport and Optical Properties of Inhomogeneous Media (North-Holland, Amsterdam, 1989).
[3] R.G. Barrera, C. Noguez and E.V. Anda, J. Chem. Phys. 96 (1992) 1574.
[4] B. Cichocki and B.U. Felderhof, J. Chem. Phys. 90 (1989) 4960.
[5] R.I. Cukier, J. Karkheck, S. Kumar and S.Y. Sheu, Phys. Rev. B 41 (1990) 1630.
[6] R.G. Barrera, M. del Castillo-Mussot, G. Monsivais, P. Villaseñor-González and W.L. Mochán, Phys. Rev. B 43 (1991) 13819.
[7] R.G. Barrera, J. Giraldo and W.L. Mochán, Phys. Rev. B 47 (1993) 8528.
[8] Z. Chen and P. Sheng, Phys. Rev. B 39 (1989) 9816.